American Journal of Mathematical and Computer Modelling
2026; 11(1): 13-29
http://www.sciencepublishinggroup.com/j/ajmcm
doi: 10.11648/j.ajmcm.20261101.12

Hiemenz Steady Hydromagnetic Flow and Heat and Mass Transfer Through a Porous Medium onto a Stretching Surface With Heat Absorption Under Chemical Reaction Effects

Deva Kanta Phukan*

Demow College(Sivasagar), Dibrugarh, Assam, India

Email address:
drdevakanta@gmail.com (Deva Kanta Phukan)
*Corresponding author

To cite this article:
Deva Kanta Phukan. (2026). Hiemenz Steady Hydromagnetic Flow and Heat and Mass Transfer Through a Porous Medium onto a Stretching Surface With Heat Absorption Under Chemical Reaction Effects . *American Journal of Mathematical and Computer Modelling, 11*(1), 13-29. https://doi.org/10.11648/j.ajmcm.20261101.12

Received: 20 October 2025; **Accepted:** 6 November 2025; **Published:** 20 January 2026

Abstract: In the present paper, steady stagnation flow of conducting fluid through a porous medium over a flat stretching surface with heat absorption/generation and chemical reaction in the presence of magnetic field has been studied under Soret and Dufour effects. The governing partial differential equation involved in this analysis viz conservation of mass, momentum, energy and concentration are transformed into self similar steady equations using similarity transformations and are solved numerically by using the Runge-Kutta fourth order scheme along with shooting technique for the whole domain for different existing flow parameters in this investigation. A representative set of graphical results for the flow field, temperature and concentration are presented for the different existing non dimensional flow parameters. The dimensionless velocity profiles are seen to decrease with increasing the magnetic, Lewis, porosity, viscosity, radiation, chemical reaction parameters and increases with Soret, Dufour, Stretching, thermal and concentration buoyancy parameters. An enhancement of temperature and concentration profiles are observed with increasing magnetic, and porosity parameter and the both temperature and concentration fall down with increment of surface stretching parameter, Prandtl number, thermal and concentration buoyancy parameters. On the other hands, the concentration is seen to become more thicker with enhancement of Soret, radiation, viscosity parameters while the reversed effects is observed in the case of temperature distribution. The reduction in concentration is observed with the increasing Lewis, Dufour, heat absorption, chemical reaction parameter and enhancement in temperature is noted for these parameters. Furthermore, the shear stress parameters, the rate of heat transfer and mass transfer are derived for existing non-dimensional flow parameters. A special case of our results obtained during investigation is an excellent agreement with an earlier published work.

Keywords: Stagnation Flow, Soret and Dufour Number, Conducting Fluid, Heat and Mass Transfer, Chemical Reaction, Heat Absorption, Magnetic Field

1. Introduction

Study of MHD flow of viscous conducting fluid with heat and mass transfer through a porous medium plays an important role in technological applications. During recent years, this fluid flow phenomena through a porous medium has been a subject of fundamental importance as it is relevant to several industrial applications such as crystal magnetic damping control, hydro-magnetic chromatography, chemical catalytic reactors, heat and mass transfer characteristic in nano -fluid for power plants, heat exchange between soil and atmosphere, packed sphere beds, and migration of moisture through the air contained in fibrous insulation and for this industrial context has drawn attention of many fluid dynamist s and applied mathematicians.

Furthermore, it is usually observed that many practical diffusive operations involve the molecular diffusion of species in the presence of a chemical reaction within or at the boundary layer. The chemical reaction occurs in two different way namely homogeneous reaction and heterogeneous reaction. A homogeneous reaction is one which occurs uniformly throughout a given phase and the species generation in a homogeneous reaction is analogous to internal source of heat generation. But a heterogeneous reaction takes place in a restricted region or within the boundary of a phase. So it may be treated as boundary condition similar to the constant heat flux condition in heat transfer. The study of simultaneous heat and mass transfer within a chemical reaction is of great practical importance for the fluid dynamist and applied mathematicians due to its almost universal occurrence in many branches of science and engineering [1]. Hiemenz discovered that stagnation point flow can be analysed using the Navier-Stokes equation for the flow field [2]. Later on, Goldstein [3] discussed the heat transfer of stagnation point flow and the temperature distributions were investigated by Sibulkin [4]. The study of boundary layer flow over a continuous solid surface moving with constant speed was presented by Sakiadis [5] and the heat transfer phenomenon of magneto-hydrodynamics Hiemenz flow under the effect of uniform suction/ injection through porous medium was studied by Yih [6]. An exhaustive volume of work devoted to the area of porous media includes the most recent books by Fairbanks and Wike [7], Das et al. [8]. Nield and Bejan [9], Vafai [10], Pop and Ingham [11] and Ingham and Pop [12]. Heat and mass transfer over an accelerating surface with heat source in the presence of suction and blowing was studied by Achary et al. [13]. El-Arabawy [14] discussed the effect of suction/ injection on the flow of a micro-polar fluid past a continuously moving plate in the presence of radiation. Attia [15] presented a similar solution for the plane flow through porous medium onto a stretching surface with internal heat source for both the momentum and energy governing equations. Kandasamy et al. [1, 16] studied the heat and mass transfer under a chemical reaction with heat source .

Chemical reaction generally associate a large amount of exothermic reactions. These characteristic can be easily seen in a lot of industrial processes. Recently, it has been established that convection effects in a porous constructed chemical reactors cannot be ignored by Seddeek et al. [17]. The reaction produce in a porous medium was extraordinarily in common, such as the topic of PEM fuel cells modules and the polluted underground water because of discharging the toxi substance etc. The thermal radiation and buoyancy effect on MHD free convection heat generation flow over an accelerating permeable surface with the influence temperature dependent viscosity was presented by Seddeek [17] and later on the effects of chemical reaction, variable viscosity, the effects of axial magnetic field, the temperature convection flow problems were included by Seddeek and Salem [18]. The boundary layer flow over a flat plate embedded in a porous medium was presented by Liao and Pop [19]. Postelnicu [20] discussed on influence of chemical reaction on heat and mass transfer by natural convection from vertical surfaces in porous media considering Soret and Dufour effects. An analysis on the MHD mixed convection flow under the radiation interaction along a vertical permeable surface immersed in a porous medium in the presence of Soret and Dufour effects was offered by Chamkha and Ben-Nakhi [21]. Tsai and Huang [22] analysed Soret and Dufour effects on Hiemenz flow for heat and mass transfer through porous medium onto a stretching surface. Sallam [23] presented the investigation on thermal diffusion and diffusion-Thermo effects on mixed convection heat and mass transfer in porous medium. Nayak et al. [24] investigated Soret and Dufour effect in a on mixed convection unsteady MHD boundary layer flow over stretching sheet in porous medium with chemically reactive species. Mohanty et al.[25] forwarded a Numerical investigation on heat and mass transfer effect of micro-polar fluid over a stretching sheet through porous media. Veerkrishna et al. [26] discussed heat and mass transfer on free convective flow of a micro-polar fluid through a porous surface with inclined magnetic field and Hall effects. Veerkrishna et al. [27] also investigated on heat and mass transfer of second grade fluid through porous medium over a semi-infinite vertical stretching sheet.An investigation on Hiemenz stagnation point flow with computational modeling of variety of boundary conditions was studied by Vishalakshi et al. [28]. Bormudoi and Ahmed [29] presented an investigation on effect of diffusion thermo on a mixed convective heat and mass transfer MHD flow through a vertical porous plate including radiation absorption. An extension on Hiemenz stagnation point flow to a tern king sheet with Brinking Model was also investigated by Vishalakshi et al. [30]. An extensive amount of studies on Soret and Dufour effects on various model of fluid flow, temperature and concentration in porous media were presented by several researchers [31, 32]. Recently, Sachhin et al. [33] investigated the effect of velocity slip and MHD on Hiemenz stagnation flow of a ternary nano fluid and heat and mass transfer.

In the present paper, we investigate the hydro-magnetic Hiemenz steady flow, and heat and mass transfer through a porous medium on to stretching surface with heat absorption chemical reaction considering thermal-diffusion and diffusion thermo-effects. The outline of the paper is as follows. In the next section, we describe the model for the flow problem considered and formulation of the problem. The numerical solution procedure of the steady problem is explained in section 3. The penultimate section presents the result graphically with proper validation of the procedure and through computing tables obtained for different existing physical parameters. Finally, the paper closes with concluding remarks.

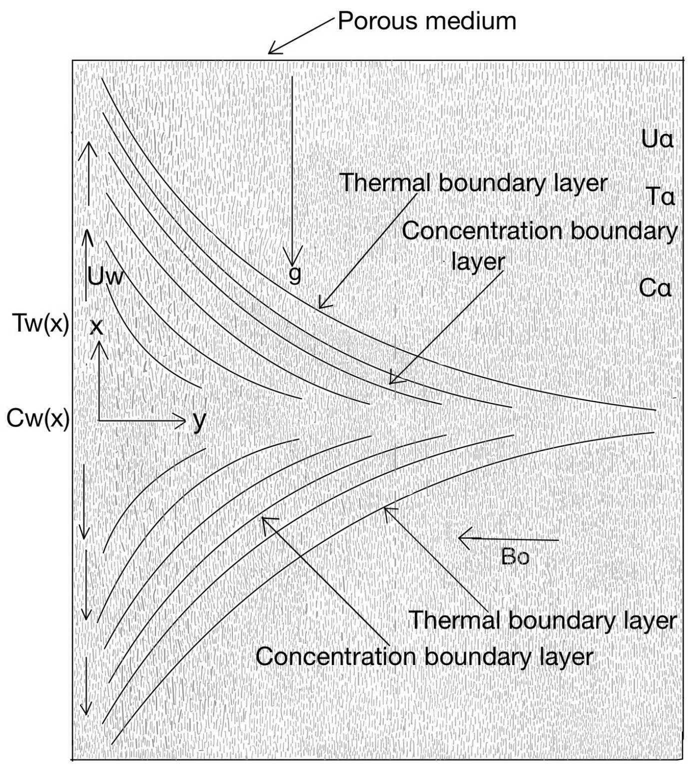

Figure 1. *Sketch of the stagnation flow model.*

2. Formulation of the Problem

The scenario of typical flow is illustrated in Figure 1 which shows the two dimensional steady state, viscous, incompressible, laminar Hiemenz flow of conducting fluid through a porous medium onto a vertical flat stretching surface with stretching rate $U_e(\infty) = ax\ a > 0$. The x-axis is taken along the stretching direction of the street and y-axis is normal to the stretching sheet. A uniform magnetic field of strength B_0 is applied in the negative direction of y-axis and the acceleration due to gravity acts in the negative direction of x-axis. It is assumed that the sheet is non-conducting and the effects of the radiating and Joule heating, the Hall effects and induced magnetic field are neglected while Soret and Dufour effects are considered. The viscosity of the fluid varies with the natural exponent and is expressed in the form $\frac{\mu}{\mu_0} = e^{-\alpha\theta}$ and μ_0 is the viscosity at temperature T_w and α is the viscosity parameter. The heat absorption or heat generation and its property variations due to temperature are limited to density and viscosity. More over, the density variation and the effects of the buoyancy are taken into consideration which could be adopted the Boussinesq approximations for both temperature and concentration gradient. In addition, the chemical reaction is taking place in the flow over the porous medium with the effective mass diffusivity D_e and the rate of chemical reaction k_l throughout the fluid. The u and v are the velocity component in the direction of x and y respectively, T and C are the temperature and concentration variables respectively.Under these assumptions, the Governing boundary layer equations of mass, momentum, energy and concentration describing the flow under the Boussinesq approximations could be written as follows

$$\frac{\partial u}{\partial x} + \frac{\partial v}{\partial y} = 0, \tag{1}$$

$$\left.\begin{aligned} u\frac{\partial u}{\partial x} + v\frac{\partial v}{\partial y} = \frac{1}{\rho}\frac{\partial}{\partial y}\left(\mu\frac{\partial u}{\partial y}\right) + U_\infty\frac{dU_\infty}{dx} + g\beta_T(T - T_\infty) \\ + g\beta_C(C - C_\infty) - \left(\frac{\nu}{K} + \frac{\sigma B_0^2}{\rho}\right)(u - U_\infty)\,, \end{aligned}\right\} \tag{2}$$

$$u\frac{\partial T}{\partial x} + v\frac{\partial T}{\partial y} = \alpha_e\frac{\partial^2 T}{\partial y^2} - \frac{1}{\rho C_p}\frac{\partial q_r}{\partial y} + \frac{Q}{\rho C_p}(T_w - T_\infty) + \frac{D_\epsilon k_T}{C_s C_p}\frac{\partial^2 C}{\partial y^2}, \tag{3}$$

and

$$u\frac{\partial C}{\partial x} + v\frac{\partial C}{\partial y} = D_e\frac{\partial^2 C}{\partial y^2} - K_l(C_w - C_\infty) + \frac{D_\epsilon k_T}{T_m}\frac{\partial^2 T}{\partial y^2}, \tag{4}$$

where μ is the viscosity, ρ is the density, σ is the electrical conductivity, α is the thermal diffusivity, ν is the kinematic viscosity, D_e is the mass diffusivity, g is the acceleration due to gravity, C_p the specific heat at constant pressure, K_T , C_s and T_m are the thermal diffusion ratio, concentration susceptibility and fluid mean temperature respectively; β_T is the thermal expansion co-efficient, β_C is the concentration expansion co-efficient, K is the permeability of the porous medium, k_l is the dimensional chemical reaction parameter, U_∞, T_∞ and C_∞ are the free stream velocity, temperature and concentration of the fluid respectively; Q is the volumetric heat absorption/generation rate, $\alpha_e(= \frac{\kappa_e}{\rho\ C_p})$ is the diffusivity of the porous medium and κ_e is the effective thermal conductivity.

The boundary conditions are given as follows

$$\left.\begin{aligned} u = U_w(x) = cx,\ v = 0,\ T = T_w(x),\ C = C_w(x)\ at\ y = 0 \\ u = U_\infty(x) = ax,\ T = T_\infty, C = C_\infty\ as\ y\ \to \infty \end{aligned}\right\}, \quad (5)$$

where the wall temperature and the concentration level at the wall are assumed as the power law variation form

$$T_w = T_\infty + C_1 x^L,\ C_w = C_\infty + C_2 x^L, \quad (6)$$

where C_1 and C_2 are constants and L is the power index of the wall temperature and species concentration, c and a are the positive constants that represents the characteristics intensity and the free stream strength respectively.

Following sparrow and Cess [8] and El-A-rabawy [14], the radiative heat flux could be expressed as

$$q_r = -\frac{4\,\sigma^*}{3\,\kappa^*}\frac{\partial T^4}{\partial y}, \quad (7)$$

where σ^* is the Stefan- Boltzman constant and κ^* is the mean absorption coefficient. If the temperature difference within the flow field is assumed to be sufficiently small, then T^4 can be approached as the linear function of temperature .

$$T^4 = 4T_\infty^3 T - 3T_\infty^4. \quad (8)$$

Differentiating equation (7) with respect to y and using equation (8) we get

$$\frac{\partial q_r}{\partial y} = -\frac{16\sigma^*}{3\kappa^*}T_\infty^3\frac{\partial^2 T}{\partial y^2}. \quad (9)$$

Following Tsai and Huang [22] we look for the solution to equation (1)-(4) of the form

$$\left.\begin{aligned} \psi = \sqrt{cx\nu}f(\eta),\ u = \frac{\partial\psi}{\partial y} = cxf'(\eta), v = -\frac{\partial\psi}{\partial x} = -\sqrt{c\nu}f(\eta) \\ \eta = \sqrt{\frac{c}{\nu}}\,y, \theta(\eta) = \frac{T - T_\infty}{T_w - T_\infty},\ \phi(\eta) = \frac{C - C_\infty}{C_w - C_\infty} \end{aligned}\right\}, \quad (10)$$

where prime denotes partial differentiation with respect to η. It can be noted that equation (10) is compatible with equation (1).That is, equation of continuity is satisfied for the aforesaid assumptions. Introducing the similarity transformation i.e. using equation (9) and (10), the governing partial differential equation (2)-(4) can be transformed in to a set of non-linear coupled ordinary differential equation in terms of $f(\eta)$, $\theta(\eta)$ and $\phi(\eta)$ could be expressed as

$$f''' + (f - \alpha\,\theta')f'' + S^2 - f'^2 + G_r\theta + G_m\phi + \Omega(f - S) - M(f - S) = 0, \quad (11)$$

$$\frac{(R+1)}{R}\theta'' - P_r(f\theta' - Lf'\theta + Q_r\theta) + D_f\phi'' = 0 \quad (12)$$

and

$$\phi'' + P_r L_e(f\phi' - Lf'\phi - k_r\phi) + S_r L_e\phi'' = 0. \quad (13)$$

The appropriate transformed boundary conditions are given by

$$\left.\begin{aligned} f(0) = 0,\ f'(0) = 1,\ \theta(0) = 1,\ \phi(0) = 1,\ at\ \eta = 0 \\ f'(\infty) = S,\ \theta(\infty) = 0,\ \phi(\infty) = 0, as\ \eta \to \infty \end{aligned}\right\}, \quad (14)$$

where $M = \frac{\sigma B_0^2}{\rho c}$ is the magnetic parameter, $S = \frac{a}{c}$ is the stretching parameter, $\Omega = \frac{\nu}{cK}$ is the porosity parameter, $G_r = \frac{g\beta_T(T_w - T_\infty)}{cu_w}$ is the temperature buoyancy parameter, $G_m = \frac{g\beta_C(C_w - C_\infty)}{cu_w}$ is the concentration buoyancy parameter, $P_r = \frac{\mu C_p}{\kappa_e}$ is the Prandtl number, $L_e = \frac{\alpha}{D_e}$ is the Lewis number, $Q_r = \frac{Q}{c\rho C_p}$ is the heat source parameter, $R = \frac{3\kappa^* k_e}{16\sigma^* T_\infty^3}$ is the radiation parameter, $k_r = \frac{k_1}{c}$ is the chemical reaction parameter, α is the viscosity parameter, $D_f = \frac{D_e K_T(C_w - C_\infty)}{C_s C_p(T_w - T_\infty)}$ is the Dufour number and $S_r = \frac{D_e K_T(T_w - T_\infty)}{T_m\alpha_e(C_w - C_\infty)}$ is the Soret number.

3. Numerical Solution of the Problem

The governing equations (11)-(13) which are in non dimensional form represents a coupled non-linear ordinary differential equations cannot be solved analytically subject to the boundary conditions (14). Further more, a direct numerical solutions of the similarity solutions (11)-(13) cannot be obtained because in order to integrate the pair of coupled seventh order ordinary differential equations by the standard numerical method, seven conditions must be prescribed at the initial point of integration. Since there are missing three initial conditions at the initial point of integration i.e. the values of $f''(0)$, $\theta'(0)$ and $\phi'(0)$ are not prescribed at the initial point of integration. So to solve the aforesaid equations, it is required to determine the values of missing initial conditions by an appropriate numerical method. The shooting method is a suitable one which enables us to convert a boundary value problem to an initial value problem. Equations (11)-(13) with the boundary conditions (14) can be integrated numerically using the fourth order of Runge-Kutta algorithm with Newton iteration in doubled precisions with a systematic guessing of $f''(0)$, $\theta'(0)$ and $\phi'(0)$ by the shooting technique. The accuracy of the numerical results obtained for the flow field, temperature and concentration of the fluid across the boundary layer depend very much on how the guesses are chosen. If several cases for different existing parameters flow parameters are to be studied corresponding to many values of these parameters, we have to make a great number of guesses. The inherent error in the Runge-Kutta method cannot be estimated easily. Furthermore, the source of error in the simulation is noted to arise from the prescribed boundary conditions at the infinity. The main reason in this simulation is that physical domain under consideration is unbounded whereas the computational domain is finite. In fact, the far field boundary condition usually depends on the physical parameters of the problem and its value needs to be adjusted as the value of the parameters change. In practice, the computational domain is chosen to be sufficiently large, so that numerical solution closely approximate the terminal boundary conditions at infinity. In this discussion, the boundary condition at the far end has been fixed to 5 and less than 5 depending on the choice of the values of flow parameters viz. magnetic parameter M, Prandtl number P_r, Lewis number L_e, thermal Grashof number G_r, mass Grashof number G_m, stretching parameter S , radiation parameter R, the heat source parameter Q_r, Soret parameter S_r, the porosity parameter Ω, the chemical reaction parameter k_r and Dufour parameter D_f.

4. Results and Discursion

A graphical representation has been plotted to analyze the influence of various existing flow parameters on the dimensionless velocity profile $f'(\eta)$, temperature profile $\theta(\eta)$ and $\phi(\eta)$ concentration profile through graphs (see Figs.2-12). Figures 2 (a), (b), (c) show the velocity $f'(\eta)$, temperature $\theta(\eta)$and concentration profiles $\phi(\eta)$ respectively for various values of magnetic parameter M with other fixed existing flow parameters. From Figure 2 (a) it is seen that velocity starts from initial value at the surface and increase till it attain the peak value and then starts decrease until it reaches to the minimum value $S = 0.5$ at the end of the boundary layer for different magnetic parameter M and it is clear that the effect of magnetic field is to decrease the velocity throughout the boundary layer. The effect of magnetic field is more prominent at the peak point, i.e. the value at peak point drastically decreases with increase the value of magnetic parameter M , because the presence of magnetic field in an electrically conducting fluid introduces a force called Lorentz force which acts in opposite direction of the flow since the applied magnetic field is normal to the surface of the sheet. This retarding force slows down the fluid velocity as shown in Figure 2 (a) . The Figure 2 (b) shows that the increase in the value of magnetic parameter M results in the increase in the temperature due to the fact that the extra work used to drag the fluid motion against the magnetic field is dissipated in the form of thermal energy in the boundary layer. This results in heating of the boundary layer and consequently temperature increases in the boundary layer region. Figure 2 (c) shows that the concentration of the increase with the increase of magnetic parameter M. The deceleration of the flow due to the magnetic force called Lorentz force enhances the species diffusion in the boundary layer, and that results in the increase in the concentration. Thus, the results indicate that magnetic parameter M is found to have significant effect on the flow fields. Figures 3 (a), (b) , (c) show the velocity, temperature and concentration profiles respectively for various values of Lewis number L_e with other parameters fixed. Since the Lewis number L_e represents the ratio of thermal diffusivity to mass diffusivity, so the influences of Lewis number can lead to decrease in velocity (see Figure 3 (a)) in cases involving heat and mass transfer. Figure 3 (c) demonstrates that the effect of Lewis number L_e is to increase the temperature of the conducting fluid but reverse effect is observed in case of concentration profiles. That is, concentration of the species being transferred diminishes. This is due to higher indicates that heat transfer (thermal diffusivity) is more dominant than mass transfer(mass diffusivity)causing concentration boundary layer thin for which concentration decreases with increase of Lewis number L_e as shown in Figure 3 (b). The effects of Soret number S_r on the profiles of velocity, temperature and concentration are displayed in Figures 4 (a), (b), (c) respectively. It is noted that an increase in the Soret number S_r due to contribution of temperature gradients to species diffusion increases the concentration in Figure 4 (c) and consequently enhances the velocity of the fluid as in Figure 4 (a). Thus the effects of Soret parameter S_r are to increase the velocity and concentration across the boundary layer but temperature profile is seen to decrease with increase the Soret parameter S_r as seen in Figure 4 (b). The Dufour effects D_f on the velocity, temperature and concentration have been analysed in Figures 5 (a), (b), (c) respectively for fixed flow parameters. It is observed from Figures 5 (a), (b) that the velocity and temperature are seen to increase with the increase of Dufour number D_f respectively but reverse effect is observed in the case of concentration as in Figure 5 (c). Physically, Dufour parameter D_f which appears in the temperature equation measures the contribution of concentration gradient to thermal energy flux in the flow field. It plays a significant role in enhancing the flow velocity and has the ability to enhance the thermal energy in the boundary layer. That is why, temperature profile at all stages increase with increase of D_f but reverse effect is seen for the case of concentration profile i.e. concentration boundary layer becomes thinner with increase in Dufour parameter D_f. The effects of thermal and concentration buoyancy parameters G_r and G_m are displayed on dimensionless velocity, temperature and concentration in Figures 6 (a), (b), (c) respectively for $S = 0.5$. Since the buoyancy force increases and acts in the upward direction and as a result induces more flow along the vertical surface which causes the fluid velocity increase i.e. assisting the flow in the upward direction. So the effect of G_r and G_m is to increase the velocity across the boundary layer as in Figure 6 (a) for both magnetic $M = 5$ and non magnetic $M = 0$ cases. The increasing buoyancy parameters G_r and G_m indicate the larger temperature and concentration gradient from the wall to the immediate surrounding. In other words, the gradually increasing G_r and G_m make enhance the stronger buoyancy force and thus leads to the larger velocity as in Figure 6 (a). The larger velocity accompanies with the decreasing boundary layer thickness and concentration boundary layer thickness. This phenomenon occurs in sight the flow velocity at the expense of (as a compensation of) both temperature and concentration of the conducting fluid . Hence the effects of both G_r and G_m are to decrease the temperature and concentration of the fluid in Figure 6(b) and Figure 6(c) respectively for both magnetic $M = 5$ and non magnetic $M = 0$ cases. The results presented in Figures 6 (a), (b), (c) for $M = 0$ are in excellent agreement with the result of Tsai and Huang [22]. Figures 7 (a), (b), (c) represent the velocity, temperature and concentration profiles for different stretching parameter S which stands for the ratio of free stream strength compared to the stretching intensity. The effect of S is to increase the velocity across the boundary layer in Figure 7 (a), but reverse effect of S is observed for the temperature and the concentration profile in Figure 7 (b) and Figure (c) respectively. Figures 8 (a), (b), (c) display the effect of radiation parameter R on the velocity, temperature and concentration profiles across the boundary layer. It can be seen from Figures 8 (a) that the velocity profiles decrease with increasing radiation parameter R for both magnetic $M = 5$ and non magnetic $M = 0$ cases. The increase of radiation parameter R leads to decrease the boundary thickness and enhance the heat transfer rate in the presence of thermal and solutal buoyancy forces. So the velocity profile is seen to decrease with the increasing radiation parameter R. On the other hand, large values of radiation parameter R corresponds to dominance of conduction over radiation there by decreasing the buoyancy force and reducing the thickness of thermal boundary layer. Hence the temperature profile is also observed to decrease in the thermal boundary layer with increase radiation parameter R(see Figure 8 (b)) for both magnetic $M = 5$ and non magnetic $M = 0$ cases . But reversed effect of R is observed in case of concentration as displayed in Figure 8 (c). That is, concentration is seen to increase with increasing the radiation parameter R for both magnetic $M = 5$ and non magnetic $M = 0$ cases. Figures 8 (a), (b), (c) for $M = 0$ are in good agreement with the result of Tsai and Huang [22] . The parameter Q_r stands for the heat generation or absorption rate. When $Q_r > 0$ indicates heat generation whereas $Q_r < 0$ means heat absorption. So from Figure 9 (a) can realize that heat source parameter Q_r follows with the stronger heat generation and increasing the thermal boundary layer thickness. So the temperature of the fluid increases with increase the heat source parameter Q_r in the thermal boundary layer for both magnetic $M = 5$ and non magnetic $M = 0$ cases. But concentration is seen to decrease with increase in the heat source parameter Q_r for both magnetic $M = 5$ and non magnetic $M = 0$ cases as shown in Figure 9 (b).This is because, in general, the increased temperature can accelerate chemical reactions that consume the species being measured The effects of heat source parameter Q_r on temperature and concentration as seen in Figures 9 (a), (b) for $M = 0$ excellently agree with result of Tsai and Huang[22] .Figure 9 (c) shows that the velocity profiles decrease with increase the viscosity parameter α . It is due to the internal friction within the fluid, causing resistance to flow and as a result decrease the thickness of boundary layer for both magnetic $M = 5$ and non magnetic $M = 0$ case. Moreover, increased temperature reduces viscosity due to decreased intermolecular forces of the fluid particles(liquid). Conversely viscosity increases with decreasing temperature. So the effect of viscosity parameter α is to decrease the temperature of the fluid as in Figure 10 (a) for both magnetic $M = 5$ and non magnetic $M = 0$ cases. The temperature can significantly impact the viscosity of a fluid and this effect can be further influenced by concentration. So concentration increases with increase the value of viscosity parameter α as seen in Figure 10 (b). An illustration of porosity parameter Ω on the velocity, temperature and the concentration profiles are displayed in Figures 10 (c), Figures 11 (a), (b) for both magnetic $M = 5$ and non magnetic $M = 0$ case. As the porosity parameter Ω represents the amount of void space in a porous medium and so significantly influences fluid velocity, temperature and concentration. It can be seen from Figure 10 (c) that the velocity profiles decrease with increase the porosity parameter Ω. This is due to the phenomenon that as the porosity increases, the resistance to fluid motion in the porous medium decreases which means the fluid has more space to move the porous structure, as a result decrease in velocity with increase the porosity parameter. Again when the porosity parameter is increased, leads to higher temperature due to enhanced heat transfer. This is due to the fact that the increased void space provides more surface area of heat exchange, leading to a higher over all temperature. So it can be seen from Figure 11 (a) that the temperature of the fluid increases with increase of Ω across the thermal boundary layer. It can also be seen from Figure 11 (b) that effect of porosity parameter Ω is to increase the concentration profile across the concentration boundary layer. This is due to the phenomenon that when porosity parameter Ω is increased the void space increases and the increased void space allows for more solute to be distributed through the medium. Thus, porosity parameter Ω plays a significant role in determining flow characteristics and thermal behavior of fluids within porous media. The effect of Prandtl number P_r is to decrease the temperature of the fluid as shown in Figure 11 (c) as the thermal boundary layer thickness decreases with the increasing Prandtl number P_r. It can also be seen from Figure 12 (a) that concentration of the fluid decreases with the increasing Prandtl number P_r . This is because when P_r is increased then mass diffusivity is reduced and as a result concentration boundary layer becomes thinner for higher Prandtl number P_r. Figures 12 (b), (c) and Figure 13 (a) show the effects of chemical reaction parameter k_r on the velocity, temperature and concentration profiles of the fluid for both magnetic $M = 5$ and non magnetic $M = 0$ cases. It is observed from Figure 12 (b) and Figure 13 (a) that the velocity profiles and concentration profiles are seen to decrease with the increasing chemical reaction parameter k_r across the boundary layer respectively.The effect of chemical reaction parameter k_r shown in Figure 13 (a) for $M = 0$ corresponds to the result presented in [22]. Physically, the chemical reaction parameter k_r effects the velocity, temperature and concentration of the fluid by influencing the rate of heat and mass transfer. The higher chemical reaction parameter k_r suppresses concentration and can impact on velocity and temperature. In this case, chemical reaction parameter k_r suppresses the velocity and so velocity decreases with the increasing chemical reaction parameter k_r . But reverse effect of k_r is observed in case of temperature and the temperature is seen to increase with increasing chemical reaction parameter k_r across the thermal boundary layer for both magnetic $M = 5$ and non magnetic $M = 0$ cases as seen in Figure 12 (c).

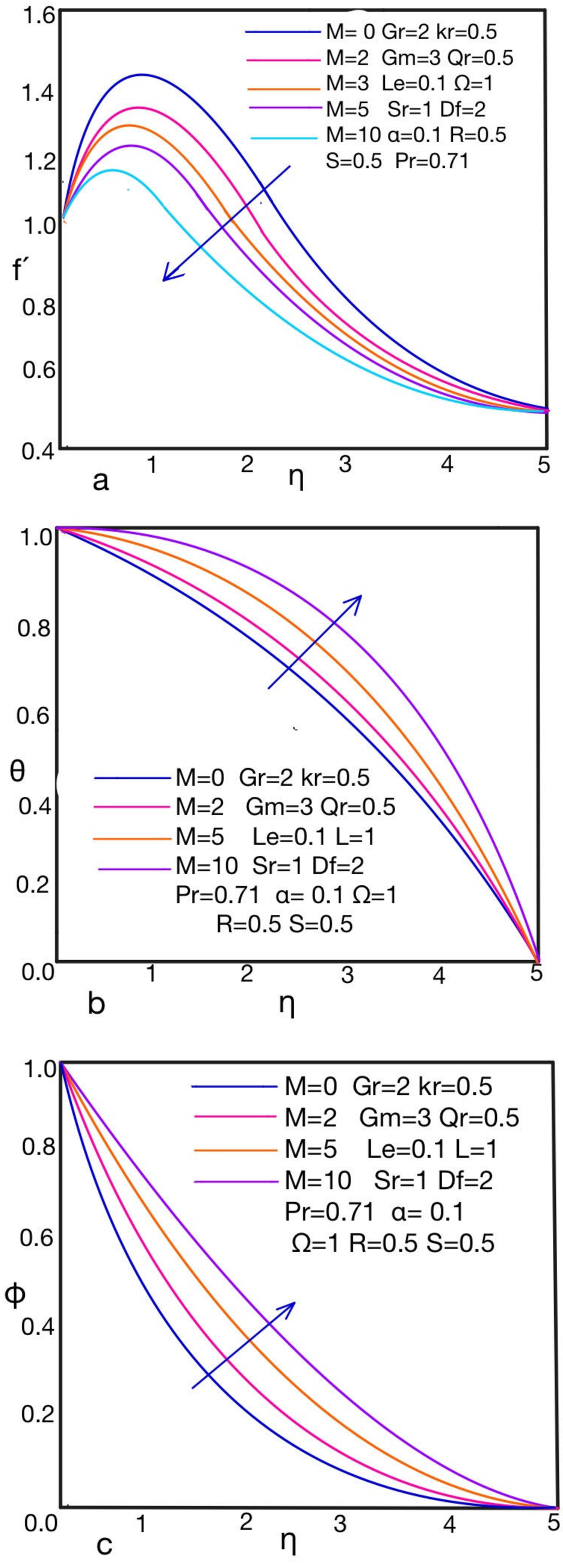

Figure 2. *a) Velocity distribution f' for different magnetic parameter M. b) Temperature distribution θ for different magnetic parameter M. c) Concentration distribution ϕ for different magnetic parameter M.*

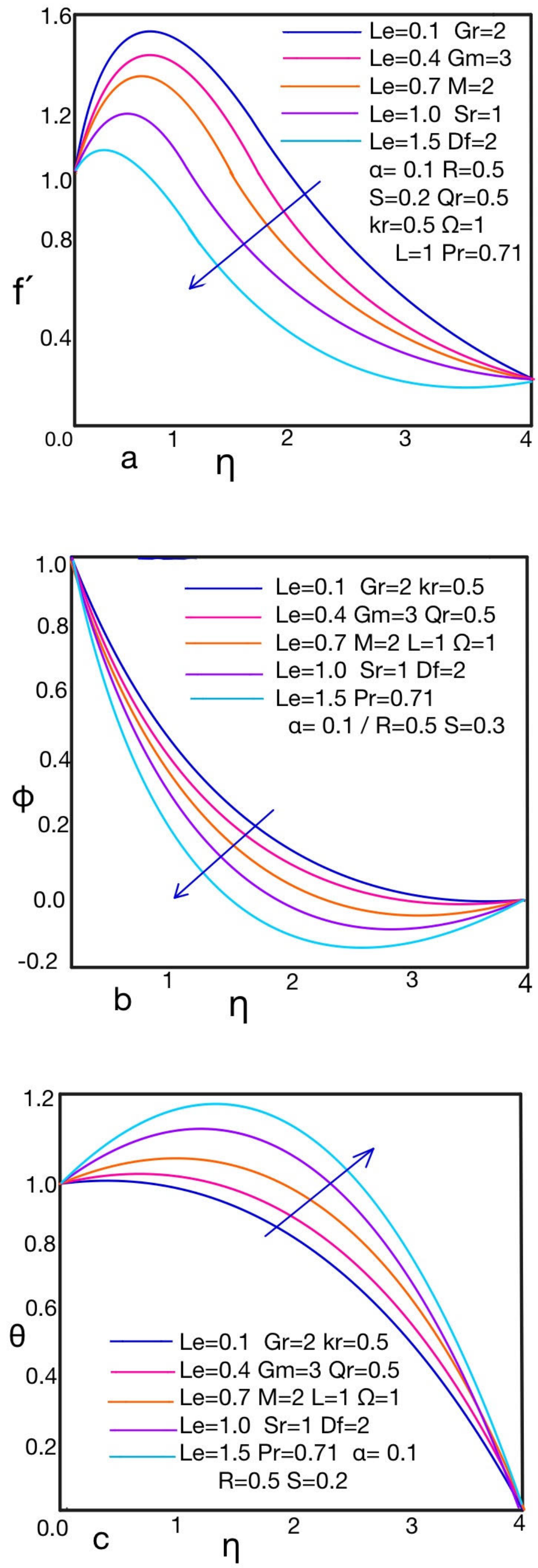

Figure 3. *a) Velocity distribution f' for different Lewis number L_e. b) Concentration distribution ϕ for different Lewis number L_e. c) Temperature distribution θ for different Lewis number L_e.*

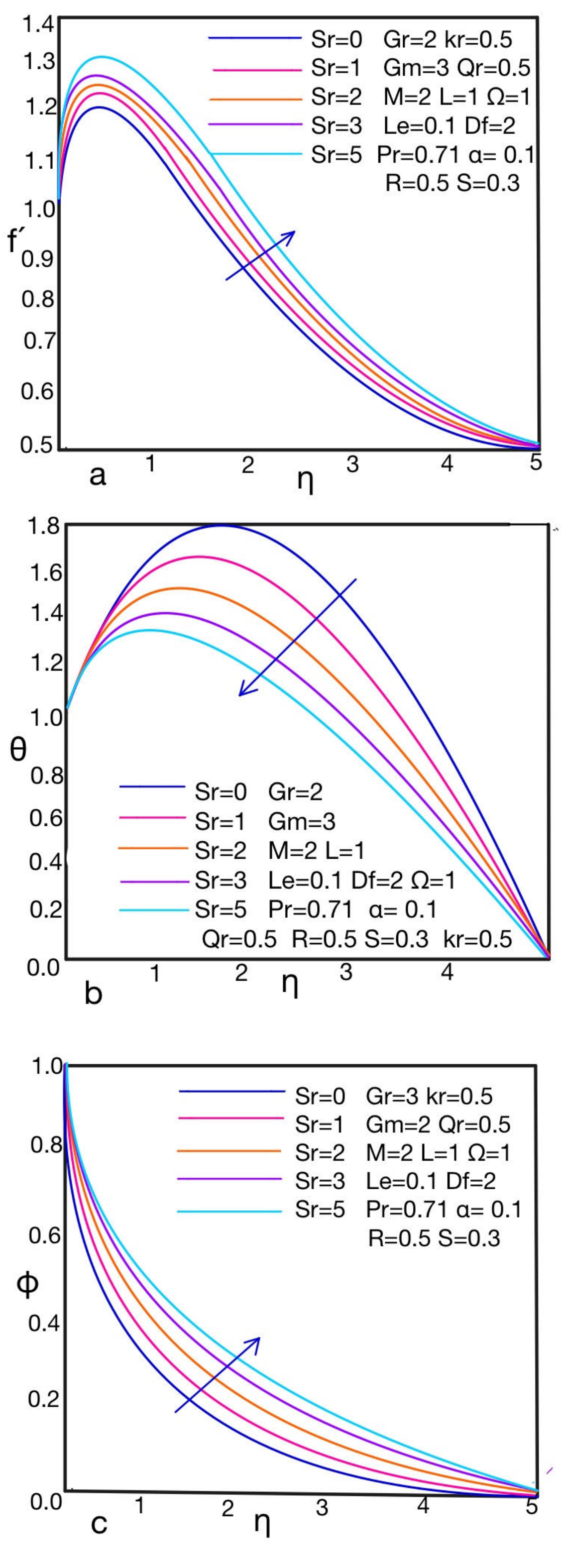

Figure 4. *a) Velocity distribution f' for different Soret number S_r. b) Temperature distribution θ for different Soret number S_r. c) Concentration distribution ϕ for different Soret number S_r.*

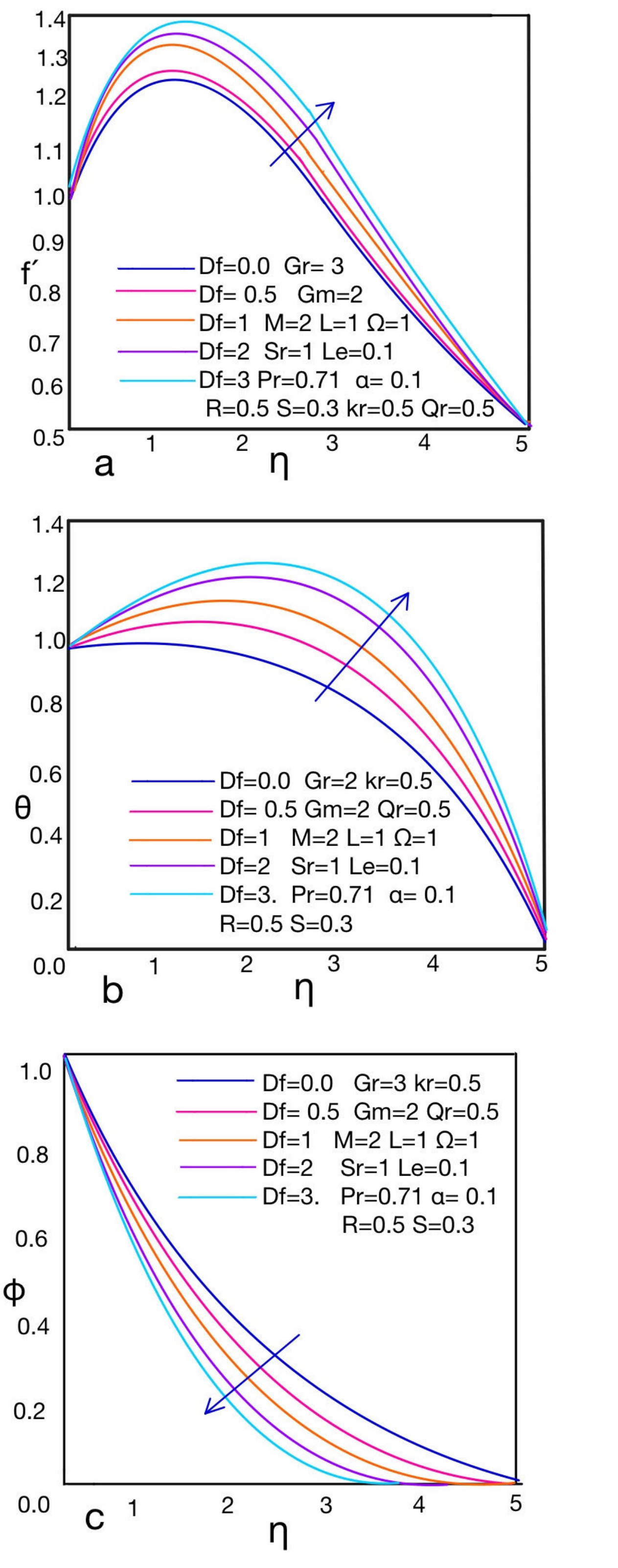

Figure 5. *a) Velocity distribution f' for different Dufour number D_f. b) Temperature distribution θ for different Dufour number D_f. c) Concentration distribution ϕ for different Dufour number D_f.*

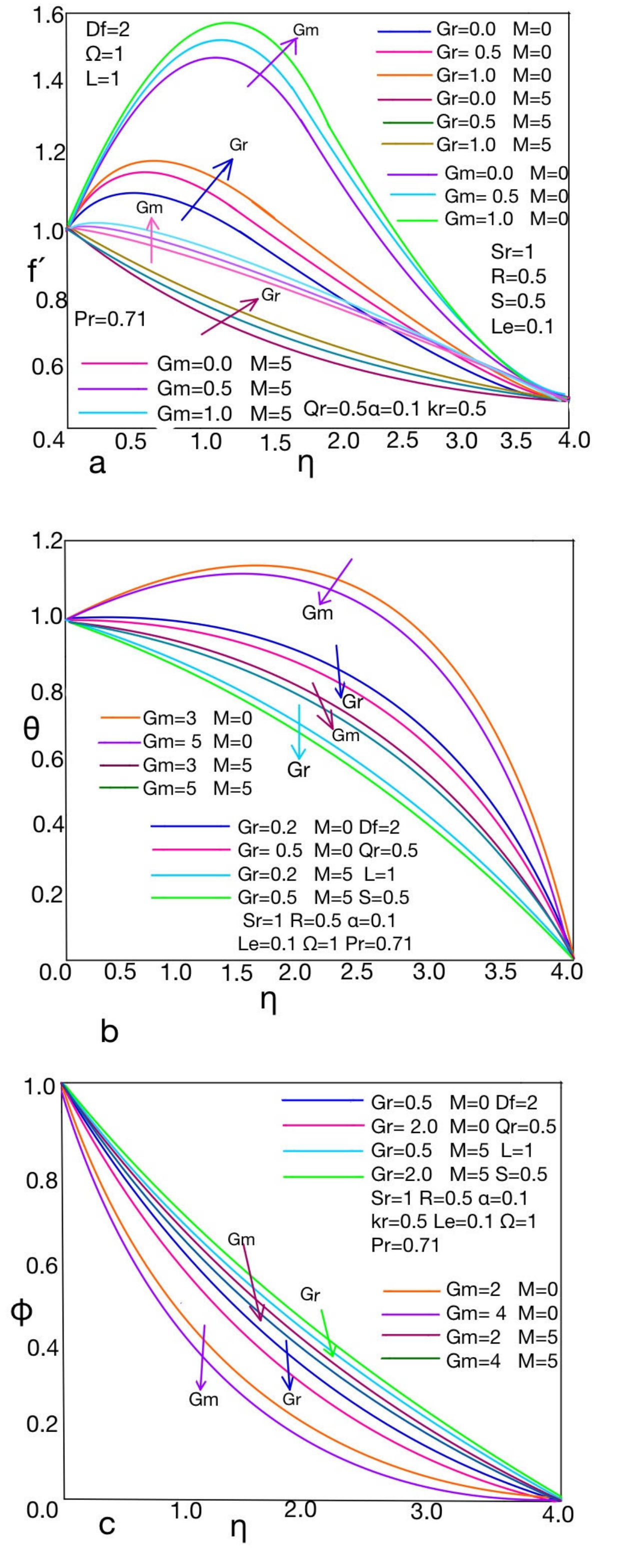

Figure 6. *a) Velocity distribution f' for different buoyancy parameter G_r and G_m. b) Temperature distribution θ for different buoyancy parameter G_r and G_m. c) Concentration distribution ϕ for different buoyancy parameter G_r and G_m.*

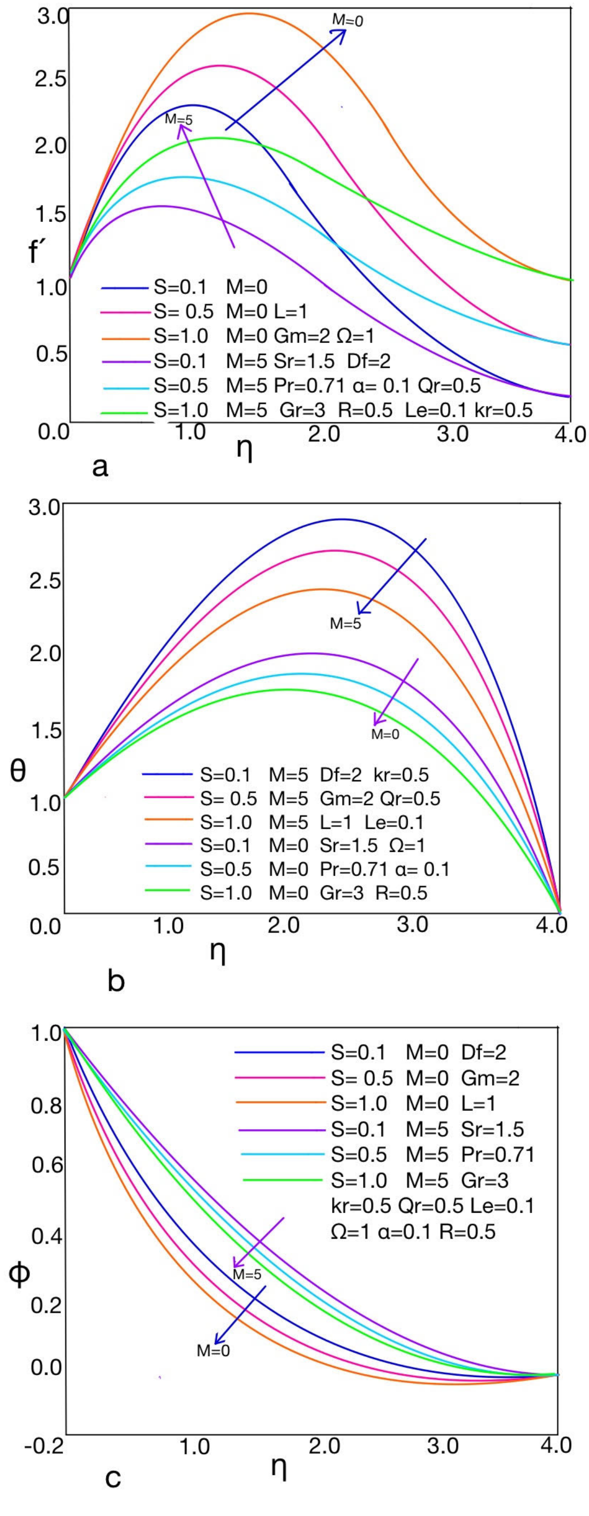

Figure 7. *a) Velocity distribution f' for different Stretching parameter S. b) Temperature distribution θ for different stretching parameter S. c) Concentration distribution ϕ for different Stretching parameter S.*

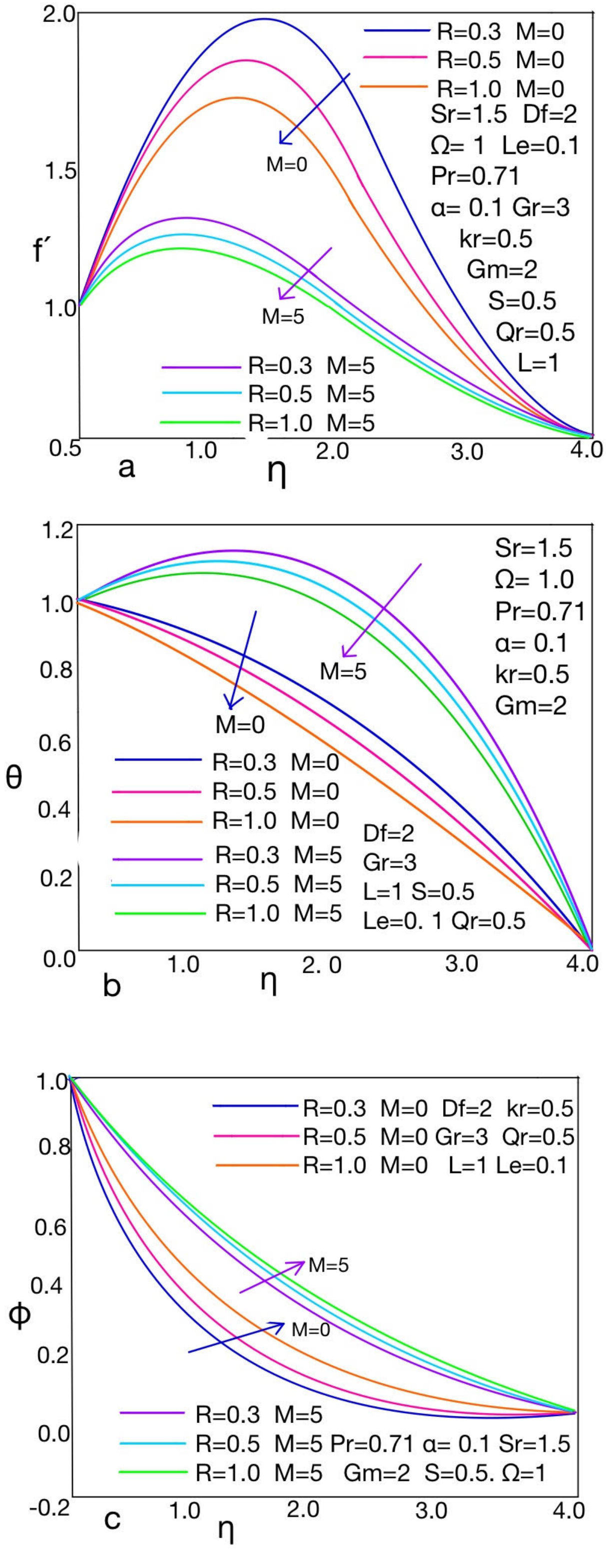

Figure 8. a) Velocity distribution f' for different Radiation parameter R. b) Temperature distribution θ for different Radiation parameter R. c) Concentration distribution ϕ for different Radiation parameter R.

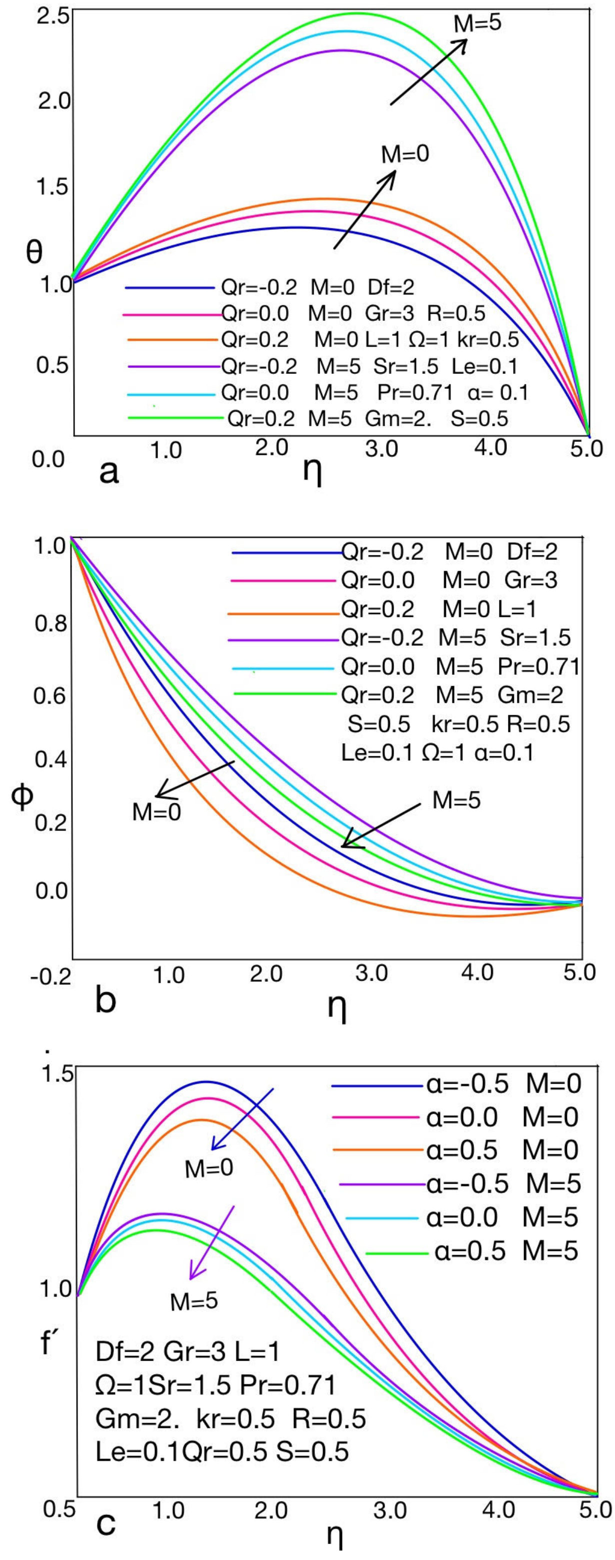

Figure 9. a) Temperature distribution θ for different heat absorption parameter Q_r. b) Concentration distribution ϕ for different stretching parameter Q_r. c) Velocity distribution f' for different viscosity parameter α.

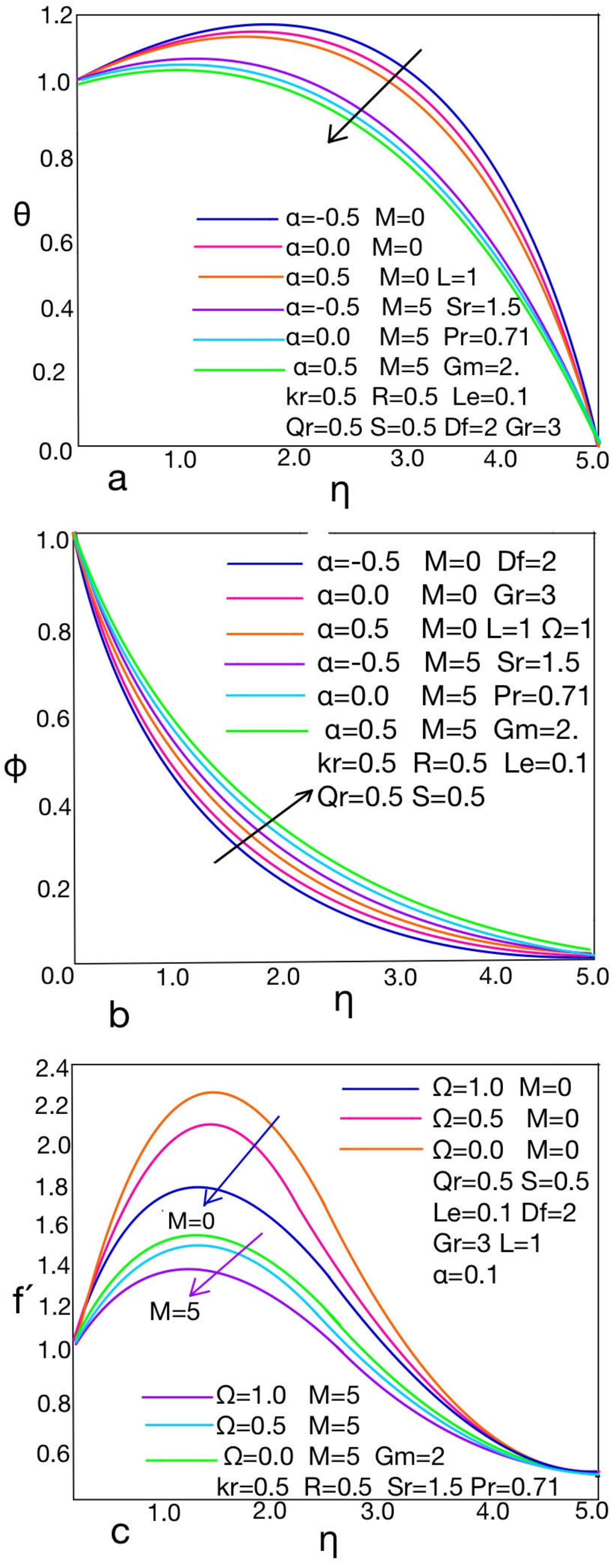

Figure 10. *a) Temperature distribution θ for different viscosity parameter α. b) Concentration distribution ϕ for different viscosity parameter α. c) Velocity distribution f' for different porosity parameter Ω.*

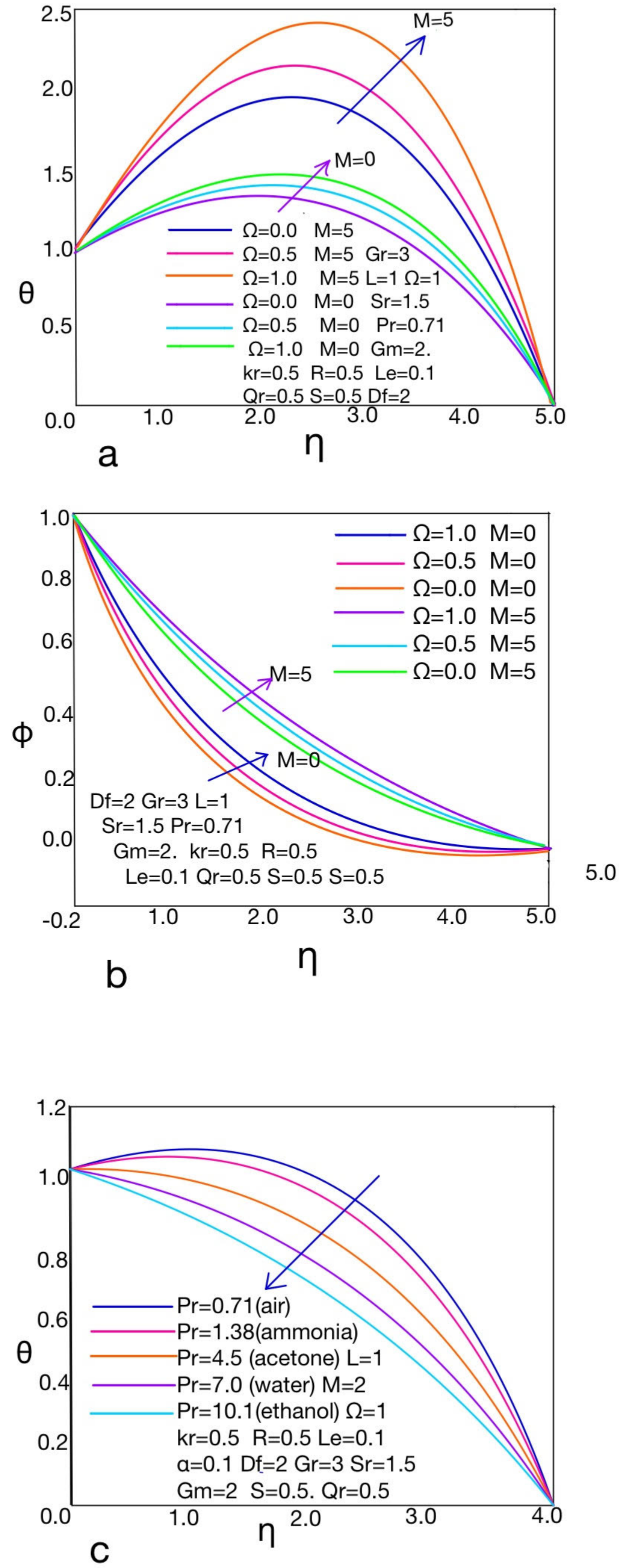

Figure 11. *a) Temperature distribution θ for different porosity parameter Ω. b) Concentration distribution ϕ for different porosity parameter Ω. c) Temperature distribution θ for different Prandtl number P_r.*

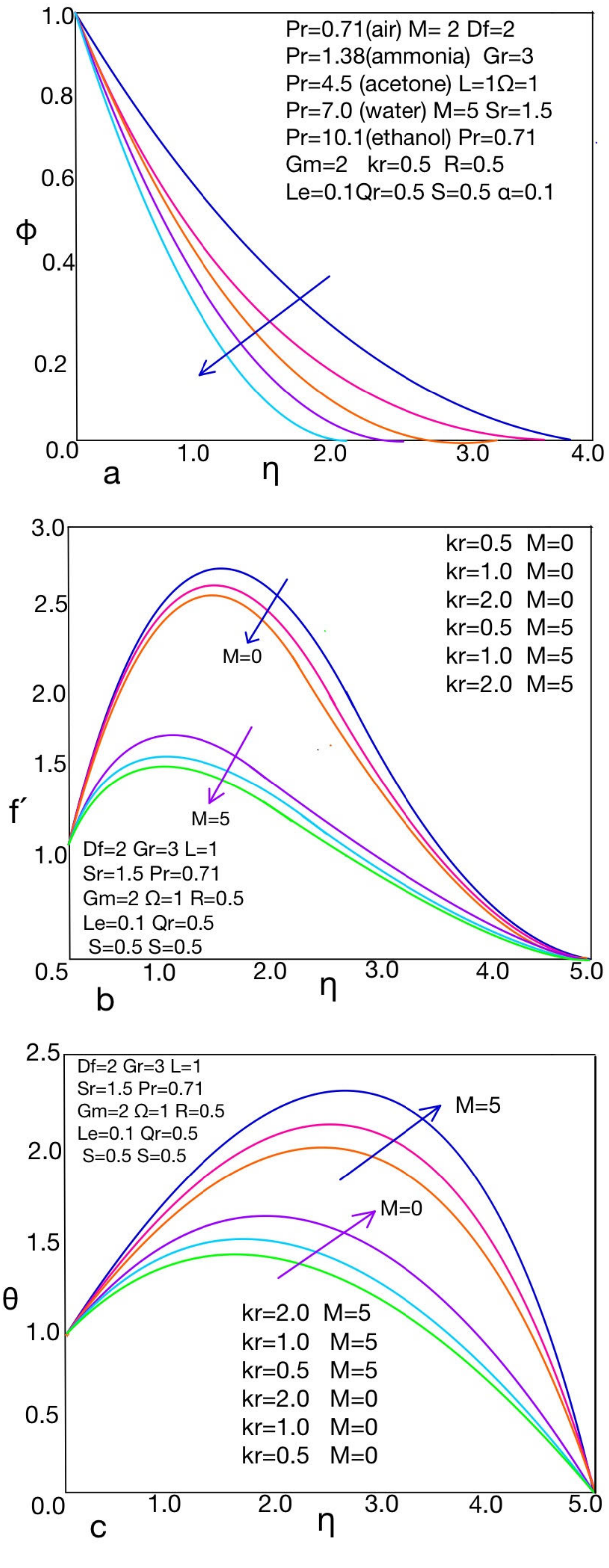

Figure 12. *a) Concentration distribution ϕ for different Prandtl number P_r. b) Velocity distribution f' for different chemical reaction parameter k_r. c) Temperature distribution θ for different chemical reaction parameter k_r.*

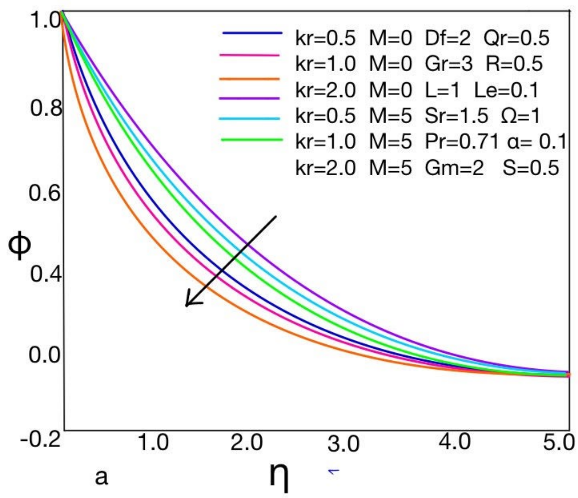

Figure 13. *a) Concentration distribution ϕ for different chemical reaction parameter k_r.*

5. Skin-friction Co-efficient, Nusselt Number and Sherwood Number

The skin-friction co-efficient, the Nusselt number and the Sherwood number have special significance for the flow, heat and mass transfer. These are important physical parameters for this type of boundary layer flow are denoted by C_f, N_u and S_h which are defined as follows [22]

$$C_f = \frac{\tau_w}{\frac{1}{2}\rho\, U_w^2} \quad where \quad \tau_w = \mu(\frac{\partial u}{\partial y})_{y=0}, \tag{15}$$

$$Nu = \frac{x\, q_w}{k_e(T_w - T_\infty)} \quad where \quad q_w = -k_e(\frac{\partial T}{\partial y})_{y=0} \tag{16}$$

and

$$Sh = \frac{x\, j_w}{D_e(C_w - C_\infty)}\, where\, j_w = -D_e(\frac{\partial C}{\partial y})_{y=0} \tag{17}$$

where μ is the co-efficient of viscosity, k_e is the effective thermal conductivity, q_w is the heat flux, j_w is the mass flux and $R_e = \frac{xu_w}{\nu}$ is the local Reynold number. Using the non-dimensional relation (10) in Equations (11)-(13), we can determine

$$C_f = 2R_e^{-\frac{1}{2}} f''(0), \tag{18}$$

$$N_u = -R_e^{-\frac{1}{2}} \theta'(0) \tag{19}$$

and

$$S_h = -R_e^{-\frac{1}{2}} \phi'(0). \tag{20}$$

The effect of magnetic parameter M on the Skin friction, Nusselt number and Sherwood numbers when the other flow parameters fixed is displayed in Table 1. It is observed that skin friction co-efficient and Nusselt number i.e. rate of heat transfer both decrease with the increasing magnetic parameter M but reversed effect is seen for the Sherwood number. The strong magnetic field reduces skin friction by creating a drag force that opposes fluid motion and also reduces Nusselt number by decreasing the convective heat transfer. This effect is particularly noticeable for the strong magnetic field and the fluid is electrically conducting. The effect of Soret parameter is seen to decrease the skin friction and Sherwood number but Nusselt number increases with the increasing Soret number in Table 2. This is due to the presence of magnetic field which exerts a force on the fluid, tending to suppress its motion and thereby reducing skin friction at the surface. In other word, increasing Soret number can decrease the Sherwood number because Soret effect can lead to a more uniform concentration distribution reducing to mass transfer rate.But the effect of Soret parameter drives the temperature gradient that leads to increases the rate oh heat transfer at the surface. So the effect of Soret number is, to decrease skin friction and Sherwood number but increase Nusselt number. The effect of Dufour number is observed to increase the skin friction and Nusselt number but opposite effect is observed in case of Sherwood number in Table 3. Increasing Dufour number leads to a rise in skin friction , resulting a greater resistance to fluid flow due to enhance momentum transfer as the strong magnetic field can amplify Dufour effect and further increase skin friction and also increase Nusselt number by reflecting a greater rate of heat transfer by convection. But Sherwood number decreases with increasing the Dufour number. Table 4 shows that thermal Grashof number influences skin friction, Nusselt number and Sherwood number. A higher Grashof number indicates stronger buoyancy forces, leading to increased velocity gradient and a potential reduction in skin friction. Again since the Nusselt number measures the rate of heat transfer at the surface and a higher thermal Grashof number generally enhances heat transfer by promoting natural convection, thus increasing Nusselt number.Thus, effect of Grashof number is to increase the skin friction and to increase rate of heat transfer (Nusselt number) at the surface. But reverse effect is seen for Sherwood number because the influence of magnetic field and porous medium might create new mass transfer mechanism. The effect of mass Grashof number is seen to increase skin Friction and Nusselt number, and is seen to decrease Sherwood number in Table 5. This is due to the fact that mass Grashof number represents the ratio of buoyancy forces to viscous forces in a concentration gradient, influences skin friction, and higher mass Grashof number tend to increase skin friction, resulting a greater frictional force between the fluid and the surface. Moreover, Nusselt number is also affected by mass Grashof number and increased mass Grashof number leads to higher Nusselt number resulting more effective heat transfer from the surface to the flow as the Nu measured the ratio of convective to conductive heat transfer.In general, Sherwood number increases with increase of mass Grashof number. But reverse effect is seen due to the presence of magnetic field and being a porous medium.The presence of magnetic field introduces additional force that can alter the flow and mass transfer characteristic and can dominant convection, potentially leading to lower Sherwood number depending on the specific flow parameters like porosity parameter etc. The effect of porosity parameter is seen to increase the Skin friction, Nusselt number and is seen to decrease the Sherwood numbers as displayed in Table 6. This is because increased porosity allows for more penetration into the porous medium, leading to greater interaction between the fluid and the surface which results a higher frictional forces, so skin friction increases with increasing the porosity parameter. Higher porosity generally promotes increased heat transfer rates because more fluid can penetrate and create a larger surface area of heat exchange. So Nusselt number increases with increasing the porosity parameter. But reverse effect is observed in case of Sherwood number. Table 7 shows that effect of Prandtl number is to increase the skin friction and Nusselt number and to decease the Sherwood number. The stretching parameter effect on skin friction, Nusselt number and Sherwood number is shown in Table 8. The effect of stretching parameter is to increase the skin friction and Nusselt number and to decease the Sherwood number.

Table 1. *The co-efficient of skin friction, rate of heat of heat transfer and rate of mass transfer for different values of M for fixed parameters* $P_r = 0.71$, $L_e = 1$, $L = 1$, $G_r = 2$, $G_m = 3$, $S = 0.5$, $R = 1.5$, $Q_r = 0.5$, $S_r = 1$, $D_f = 1$, $\Omega = 1$, $k_r = 0.6$ *and* $\alpha = 0.1$.

M	$f''(0)$	$-\theta'(0)$	$-\phi'(0)$
0	1.484216	0.956378	−2.483457
1	1.158361	0.833351	−2.340191
2	0.878068	0.737624	−2.225152
5	0.243303	0.551783	−1.993365
10	−0.445875	0.401088	−1.799595

Table 2. *The co-efficient of skin friction, rate of heat of heat transfer and rate of mass transfer for different values of* S_r *for fixed parameters* $P_r = 0.71$, $L_e = 1$, $L = 1$, $G_r = 2$, $G_m = 3$, $S = 0.5$, $R = 1.5$, $Q_r = 0.5$, $D_f = 1$, $\Omega = 1$, $k_r = 0.6$ *and* $\alpha = 0.1$.

.	$M = 0$	$M = 0$	$M = 0$	$M = 5$	$M = 5$	$M = 5$
S_r	$f''(0)$	$-\theta'(0)$	$-\phi'(0)$	$f''(0)$	$-\theta'(0)$	$-\phi'(0)$
0.1	2.5607	0.9210	−1.05656	0.5637	0.3339	−0.9182
0.2	2.5452	0.9369	−1.0877	0.5599	0.3427	−0.9342
0.5	2.4975	0.9824	−1.1801	0.5484	0.3686	−0.9817
1.0	2.4152	1.0506	−1.3293	0.5292	0.4106	−1.0596
1.5	2.2466	1.1570	−1.6014	0.4913	0.4894	−1.2097

Table 3. *The co-efficient of skin friction, rate of heat of heat transfer and rate of mass transfer for different values of* D_f *in magnetic for fixed parameters* $P_r = 0.71$, $L_e = 1$, $L = 1$, $G_r = 2$, $G_m = 3$, $S = 0.5$, $R = 1.5$, $Q_r = 0.5$, $S_r = 1$, $\Omega = 1$, $k_r = 0.6$ *and* $\alpha = 0.1$.

.	$M = 0$	$M = 0$	$M = 0$	$M = 5$	$M = 5$	$M = 5$
Df	$f''(0)$	$-\theta'(0)$	$-\phi'(0)$	$f''(0)$	$-\theta'(0)$	$-\phi'(0)$
0.1	1.3206	0.2458	−2.2957	0.1675	0.0551	−1.9228
0.2	1.3567	0.4094	−2.3371	0.1853	0.1749	−1.9396
0.5	1.4842	0.9563	−2.4834	0.2433	0.551783	−1.9933
1.0	1.7879	2.1758	−2.8565	0.3626	1.2518	−2.1012

Table 4. *The co-efficient of skin friction, rate of heat of heat transfer and rate of mass transfer for different values of* G_r *for fixed parameters* $P_r = 0.71$, $L_e = 1$, $L = 1$, $S_r = 1$, $G_m = 3$, $S = 0.5$, $R = 1.5$, $Q_r = 0.5$, $D_f = 1$, $\Omega = 1$, $k_r = 0.6$, *and* $\alpha = 0.1$.

.	$M = 0$	$M = 0$	$M = 0$	$M = 5$	$M = 5$	$M = 5$
G_r	$f''(0)$	$-\theta'(0)$	$-\phi'(0)$	$f''(0)$	$-\theta'(0)$	$-\phi'(0)$
0.1	2.5607	0.9210	−1.0565	0.5637	0.3339	−0.9182
0.5	2.4975	0.9824	−1.1801	0.5484	0.3686	−0.9817
1.0	2.4152	1.0506	−1.3293	0.5292	0.4106	−1.0596
1.5	2.2466	1.1570	−1.6014	0.4913	0.4894	−1.2097

Table 5. *The co-efficient of skin friction, rate of heat of heat transfer and rate of mass transfer for different values of* G_m *for fixed parameters* $P_r = 0.71$, $L_e = 1$, $L = 1$, $S_r = 1$, $G_r = 2$, $S = 0.5$, $R = 1.5$, $Q_r = 0.5$, $D_f = 1$, $\Omega = 1$, $k_r = 0.6$ *and* $\alpha = 0.1$.

.	$M = 0$	$M = 0$	$M = 0$	$M = 5$	$M = 5$	$M = 5$
G_m	$f''(0)$	$-\theta'(0)$	$-\phi'(0)$	$f''(0)$	$-\theta'(0)$	$-\phi'(0)$
1	1.551	0.4344	−1.1048	−0.0648	0.1524	−0.9460
2	1.9018	0.4778	−1.1261	0.2217	0.1807	−0.9641
3	2.2377	0.5059	−1.1454	0.5025	0.2077	−0.9813
5	2.8758	0.5660	−1.1796	1.0400	0.2571	−1.0118

Table 6. *The co-efficient of skin friction, rate of heat of heat transfer and rate of mass transfer for different values of* Ω *for fixed parameters* $P_r = 0.71$, $L_e = 1$, $L = 1$, $S_r = 1$, $G_m = 3$, $S = 0.5$, $R = 1.5$, $Q_r = 0.5$, $D_f = 1$, $G_r = 2$, $k_r = 0.6$ *and* $\alpha = 0.1$.

Ω	$f''(0)$	$-\theta'(0)$	$-\phi'(0)$	$f''(0)$	$-\theta'(0)$	$-\phi'(0)$
0.001	1.7364	0.4098	−1.0960	0.3023	0.1809	−0.9649
0.1	1.7817	0.4181	−1.1005	0.3210	0.1834	−0.9664
0.5	1.9667	0.4535	−1.1184	0.3990	0.1936	−0.9727
1.0	2.2377	0.5059	−1.1454	0.5025	0.2077	−0.9813

Table 7. *The co-efficient of skin friction, rate of heat of heat transfer and rate of mass transfer for different values of* P_r *for fixed parameters* $\Omega = 1$, $L_e = 1$, $L = 1$, $S_r = 1$, $G_m = 3$, $S = 0.5$, $R = 1.5$, $Q_r = 0.5$, $D_f = 1$, $G_r = 2$, $k_r = 0.6$ *and* $\alpha = 0.1$.

.	$M = 0$	$M = 0$	$M = 0$	$M = 5$	$M = 5$	$M = 5$
P_r	$f''(0)$	$-\theta'(0)$	$-\phi'(0)$	$f''(0)$	$-\theta'(0)$	$-\phi'(0)$
0.5	2.215	0.2353	−0.9549	0.5088	0.0382	−0.8318
0.71	2.2361	0.4927	−1.1367	0.5052	0.1998	−0.9745
1.0	2.3106	0.9170	−1.3945	0.5012	0.4356	−1.1676

Table 8. The co-efficient of skin friction, rate of heat of heat transfer and rate of mass transfer for different values of S for fixed parameters $P_r = 0.71$, $L_e = 1$, $L = 1$, $S_r = 1$, $G_m = 3$, $\Omega = 1$, $R = 1.5$, $Q_r = 0.5$, $D_f = 1$, $G_r = 2$, $k_r = 0.6$ and $\alpha = 0.1$.

.	$M = 0$	$M = 0$	$M = 0$	$M = 5$	$M = 5$	$M = 5$
S	$f''(0)$	$-\theta'(0)$	$-\phi'(0)$	$f''(0)$	$-\theta'(0)$	$-\phi'(0)$
0.5	2.237	0.5059	−1.1454	0.5025	0.2077	−0.9813
1.0	2.5904	0.6508	−1.2051	1.6489	0.4330	−1.0997
1.5	3.2379	0.8792	−1.2925	2.9564	0.7144	−1.2262

6. Concluding Remarks

In this problem we have studied the hydromagnetic steady Hiemenz stagnation flow and heat and mass transfer through a porous medium onto a stretching surface with heat absorption in the presence of chemical reaction. The governing partial differential equations were transformed into dimensionless coupled non-linear ordinary differential equations with appropriate boundary conditions and are solved by integrating using Runge-Kutta method accompanied with the shooting technique.

1. The dimensionless velocity profiles are observed to reduce across the boundary layer with increasing the magnetic parameter M, Lewis number L_e, radiation parameter R, viscosity parameter α, porosity parameter Ω and chemical reaction parameter k_r , and the same velocity profiles are seen to increase with increasing the thermal Grashof number G_r and mass Grashof number G_m, Soret number S_r, stretching parameter S and Dufour numbers D_f across the boundary layer. number
2. The dimensionless temperature profiles are observed to decrease with increasing the P_r, S_r, G_r, G_m, S, R, α and the temperature are observed to increase with increasing the M, L_e, D_f, Q_r, Ω and k_r across the boundary layer.
3. The dimensionless concentration profiles of the conducting fluid is reduced with increasing L_e, D_f, G_r, G_m, S, Q_r, P_r and k_r but concentration increases with increasing the M, S_r, R, α and Ω.
4. Skin friction is observed to increase with the increasing D_f, Ω G_m , P_r and S and the same skin friction decreases with the increasing M, S_r and G_r.
5. Nusselt number N_u is observed to decrease with increasing M, but reverse effect is seen for Sherwood number S_h.
6. Sherwood number S_h increases with increasing the M.
7. Nusselt number N_u is also observed to increase with increasing the S_r, D_f, G_r, G_m, S, and Ω, but reverse effect is observed in case of S_h for the aforesaid physical flow parameters.

Abbreviations

a	Free Stream Strength
B_0	Uniform Magnetic Field
c	Characteristic Stretching Coefficient
C_1, C_2	Positive Constants
C	Concentration
C_w	Concentration at the Wall
C_∞	Concentration at Free Stream
C_p	Specific Heat at Constant Pressure
C_s	Concentration Susceptibility
C_f	Skin-friction
D_e	Co-efficient of Mass Diffusivity
D_f	Dufour Number
e	Natural Exponent
f	Dimensionless Flow Stream Function
g	Acceleration Due to Gravity
G_r	Thermal Buoyancy Parameter
G_m	Concentration Buoyancy Parameter
j_w	Mass Flux
K	Permeability of Porous Medium
k_e	Effective Thermal Conductivity
K_T	Thermal-diffusion Ratio
k^*	Rosseland Mean Absorption Coefficient
k_l	Rate of Chemical Reaction
k_r	Chemical Reaction Parameter
L	Power Index
L_e	Lewis Number
M	Magnetic Field Parameter
N_u	Nusselt Number
P_r	Prandtl Number
Q	Volumetric Rate of Heat Generation/Absorption
Q_r	Heat Source Parameter
q	Heat Flux
q_r	Radiative Heat Flux
q_w	Heat Flux
R	Radiation Parameter
R_e	Reynold Number
S	Stretching Parameter
S_h	Sherwood Number
S_r	Soret Number
T	Temperature
T_w	Temperature at the Wall
T_∞	Temperature at the Free Stream
T_m	Mean Temperature of the Fluid
(U, V)	the Velocity Component for the Potential Flow
U_∞	Free Stream Velocity
U_w	Velocity at the Wall
(u, v)	Components for the Potential of Velocity at any Point (x, y)
v_0	Suction/Injection Velocity

(x, y)	Cartesian Co-ordinates
α	Viscosity Parameter
α_e	Effective Thermal Diffusivity
β_C	Concentration Expansion Co-efficient
β_T	Thermal Expansion Co-efficient
η	Dimensionless Normal Distance or Similarity Parameter
ρ	Density of Fluid
σ	Electrical Conductivity of the Fluid
σ^*	Stefan- Boltzman constant
μ	Dynamic Viscosity
μ_0	Viscosity at Wall Temperature
ν	Kinematic Viscosity
θ	Dimensionless Temperature
ϕ	Dimensionless Concentration
ψ	Stream Function
Ω	Porosity Parameter
τ_w	Co-efficient of Skin Friction
$'$	Differentiation with Respect to η
w	Wall Condition
∞	Free Stream Condition

Acknowledgments

The author is very much thankful and grateful to the reviewers and editors for their constructive and valuable suggestions for improvement this manuscripts during revision for publication in American journal of Mathematical and Computer Modeling.

Author Contributions

Deva Kanta Phukan is the sole author. The author read and approved the final manuscript.

Conflicts of Interest

The author declares no conflicts of interest.

References

[1] Kandasamy, R., Periasamy, K. and Sivagnana Prabhu, K. K. (2005). Chemical reaction, heat and mass transfer on MHD flow over a vertical stretching surface with heat source and thermal stratification effects. Int. J. Heat Mass Transfer, 48 : 4557-4561.

[2] White, F. M. (1991). Viscous fluid flow. Second ed., McGraw-Hill, New York.

[3] Goldstein, S. (1938). Modern Developments in fluid dynamics. Clarendon Press, Oxford, 1938.

[4] Sibulkin, M. (1952). Heat transfer at the rear and forward stagnation points of a body of revolution. J. Aeronaut Sci., 19 : 570-577.

[5] Sakiadis, B. C. (1961). Boundary layer behaviour on continuous solid surfaces: I. Boundary layer equations for two dimensional and axi- symmetric flow. AIChE J., 7(1): 26-28.

[6] Yih, K. A. (1998). The effects of uniform suction/ blowing on heat transfer of magneto-hydrodynamic Hiemenz flow through porous media. Acta Mech., 130: 147-158.

[7] Fairbanks, D. F. and Wike, C. R. (1950). Diffusion and chemical reaction in an isothermal laminar flow along a soluble flat plate. Ind. Eng. Chem. Res., 42: 471-475.

[8] Sparrow, E. M. and Cess, R. D. (1970). Radiation Heat Transfer. Brooks/Cole, Belmont, California.

[9] Das, U. N., Deka, R. and Soundalgekar, V. M. (1994). Effects of mass transfer on flow past an impulsive started infinite vertical plate with constant heat flux and and chemical reaction. Forsch Ingenieurwesen Eng. Res. Bd , 60: 284-289.

[10] Nield, D. A. and Bejan, A. (1999). Convection in porous media. Second Ed. Springer, Berlin.

[11] Pop, I. and Ingham, D. (2001). Convective Heat Transfer: Mathematical and Computational Modelling of Viscous Fluids and Porous Media. Pergamon, Oxford.

[12] Ingham, D. and Pop, I. (1998-2002). Transport Phenomena in porous media, Vol. 2 Pergamon, Oxford.

[13] Acharya, M. Singh, L. P. and Dash, G. C. (1999). Heat and mass transfer on an accelerating surface subjected to both power law surface temperature and power Law heat flux variations with temperature dependent heat source in the presence of suction and injection. Int. J. Engg. Sci., 37: 189-211.

[14] El-Arabawy, H. A. M. (2003). Effect of suction/ injection on the flow of a micropolar fluid past a continuousy moving plate in the presence of radiation. Int. J. Heat Mass Transfer, 46: 1471-1477.

[15] Attia, H. A. (2007). On the effectiveness of porosity on stagnation point flow towards a stretching surface with heat generation. Comput. Mater. Sci.,38: 741-745.

[16] Kandasamy, R., Periasamy, K. and Sivagnana Prabhu, K. K. (2005). Effect of Chemical reaction, heat and mass transfer along a wedge with heat source and concentration in the presence of suction or injection. Int. J. Heat Mass Transfer, 48: 1388-1394.

[17] Seddeek, M. A. (2001). Thermal radiation and buoyancy effects on MHD free convection heat generation flow over an accelerating permeable surface with temperature dependent viscosity. Can. J. Phys., 79: 725-732.

[18] Seddeek, M. A. and Salem, A.M. (2007). The effect of an axial magnetic field on the flow and heat transfer about a fluid underlying the axi-symmetric spreading surface with temperature with temperature dependent viscosity and thermal diffusivity. Comput. Mech., 39: 401-408.

[19] Liao, S. J. and Pop, I. (2004). Explicit analytic solution for similarity boundary layer equations. Int. J. Heat Mass Transfer, 47: 75-85.

[20] Postelnicu, A. (2007), Influence of chemical reaction on heat and mass transfer by natural convection from vertical surfaces in porous media considering Soret and Dufour effects. Heat Mass Transfer, 43: 595-602.

[21] Chamkha, A. J. and Ben-Nakhi, A. (2008). MHD mixed convection âradiation interaction along a permeable surface immersed in a porous medium in the presence of Soret and Dufour effect. Heat Mass transfer, 4 : 845-856.

[22] Tsai, R. and Huang, J. S. (2009). Heat and mass transfer for Soret and Dufourâs effects on Hiemenz flow through porous medium onto a stretching surface. Int. J. Heat Mass Transfer, 52: 2399-2406.

[23] Sallam, N. (2010). Thermal diffusion and diffusion-Thermo effects on mixed convection heat and mass transfer in porous medium. Journal of Porous Media, 13(4): 331-345.

[24] Nayak, A., Panda, S. and Phukan, D. K. (2014). Soret and Dufour effect in a on mixed convection unsteady MHD boundary layer flow over stretching sheet in porous medium with chemically reactive species. Appl. Math. Mech.-Engl. Ed., 35(7): 849-862. https://doi.org/10.1007/s10483-014-1830-9

[25] B. Mohanty, B., Mishra, S. R. and Pattanayak, H. B. (2015 June). Numerical investigation on heat and mass transfer effect of micro-polar fluid over a stretching sheet through porous media. Alexandria Engineering Journal, 54(2): 223-232.

[26] Veerkrishna, M., Anand, P. V. S. and Chamkha, A. J. (2019). Heat and mass transfer on free convective flow of a micro-polar fluid through a porous surface with inclined magnetic field and Hall effects. J. Porous Media, 19(3): 203–223.

[27] M. Veerkrishna, K. Jyothi, and A. J. Chamkha, (2020). Heat and mass transfer of second grade fluid through porous medium over a semi-infinite vertical stretching sheet. J. Porous Media, 23(8): 751–765. https://doi.org/10.1615/JPorMedia.2020023817

[28] Vishalakshi, A. B., Mahabaleshwar, U. S., Perez, L. M. and Manca, O. (2023 June). Hiemenz stagnation point flow with computational modelling of variety of boundary conditions. Journal of Magnetism and Magnetic Materials, 575(1): 170747.

[29] Bormudoi, M. and Ahmed, N. (2023). Effect of diffusion thermo on a mixed convective heat and mass transfer MHD flow through a vertical porous plate including radiation absorption. J. Appl. Math. Mech. (ZAMM), 1-16. https://doi.org/10.1002/zamm.202300009

[30] Vishalakshi, A. B., Vanitha, G. P., Mahabaleshwar, U. S., Botmart, T., Oztop, H. F. and Abu-Hamdeh, N. (2024). Hiemenz stagnation point flow of a ternary nanofluid and heat transfer due to porous stretching /Shrinking sheet with Brinkman Model. Journal of porous media, 27(2): 1-19. https://doi.org/10.1615/JPorMedia.2023047575

[31] Kandagal, M. and Kampepatti, R. (2024). An investigation of the heat and mass transfer effects in vertical channels with immersible fluid flow through a porous matrix. J. Appl. Math. Mech. (ZAMM) 104(10). https://doi.org/10.1002/zamm.202300998

[32] Phukan, D. K. (2025). Heat and Mass transfer under the effects of Soret and Dufour parameters of free convective Flow Past a vertical porous surface in the presence of Magnetic Field. Int. J. Theo. Appl. Math., 11(2): 34-44.

[33] Sachhin, S. M., Zeidan, D., Sang W. Joo and Manca, O. (2025). An effect of velocity slip and MHD on Hiemenz stagnation flow of ternary nano-fluid with heat and mass transfer. Journal of Thermal Analysis and Calorimetry, 150, 2533-2553.